Dissociation of a Product of a Surface Reaction in the Gas Phase: XeF_2 Reaction with Si

R. C. Hefty, J. R. Holt, M. R. Tate, D. B. Gosalvez, M. F. Bertino, and S. T. Ceyer
Department of Chemistry, Massachusetts Institute of Technology, Cambridge, Massachusetts 02139, USA
(Received 20 September 2003; published 5 May 2004)

Xenon difluoride interacts with Si(100)2 × 1 by atom abstraction, whereby a dangling bond abstracts a F atom from XeF_2, scattering the complementary XeF. Partitioning of the reaction exothermicity produces sufficient XeF rovibrational excitation for dissociation to occur. The resulting F and Xe atoms are shown to arise from dissociation of XeF in the gas phase by demonstrating that the angle-resolved velocity distributions of F, Xe, and XeF conserve momentum, energy, and mass. This experiment documents the first observation of dissociation of a surface reaction product in the gas phase.

DOI: 10.1103/PhysRevLett.92.188302 PACS numbers: 82.65.+r, 34.50.Lf, 68.47.Fg, 81.65.Cf

Molecular F_2 has been recently shown to dissociate on Si(100)2 × 1 by an atom abstraction mechanism [1–3]. This mechanism is distinct from that of classic dissociative chemisorption because a bond of an incident molecule is cleaved upon formation of only a single bond to the surface. Atom abstraction is likely in other chemisorption systems [4–6]. Here, we report XeF_2, a linear molecule, interacts with Si(100) by atom abstraction as evidenced by detection, with a triply differentially pumped, rotatable mass spectrometer in a molecular-beam surface scattering UHV apparatus [7], of the scattered, complementary XeF fragment. More importantly, some scattered XeF is sufficiently excited internally to dissociate in the gas phase before reaching the detector, producing a F and a Xe atom. The F and Xe atoms are shown conclusively to result from dissociation of XeF in the gas phase by demonstrating that the measured velocity distributions of F, Xe, and XeF conserve momentum and energy and that the number of scattered F atoms equals that of Xe. This experiment shows for the first time that a product of a surface chemical reaction can undergo dissociation in the gas phase as a result of partitioning of the exothermicity of a surface reaction.

The doubly differentially pumped XeF_2 beam is formed by expansion through a Teflon nozzle, resulting in an average energy of 1.4 kcal/mol. The velocities of the incident and scattered beams are determined by cross correlation time-of-flight (TOF) methods. The beam is incident at 20° from the normal on a *p*-type Si(100) crystal that is held at 150 K. The Si surface purity, structure, and fluorine coverage are determined as previously described [2,8,9].

Identification of the atom abstraction mechanism by detection of the scattered XeF fragment is complicated by the dissociative ionization of unreactively scattered XeF_2 to produce both XeF_2^+ ($m/e = 167$) and XeF^+ ($m/e = 148$) ions upon electron bombardment ionization in the mass spectrometer. However, TOF spectroscopy unambiguously distinguishes between XeF^+ arising from XeF radicals and XeF^+ arising from the cracking of XeF_2 on the basis of the different velocities with which a XeF radical and a XeF_2 molecule scatter from the surface [2,10]. In addition, because the fragmentation ratio, XeF^+/XeF_2^+, is known from analysis of the incident beam, the contribution of XeF_2 to the $m/e = 148$ TOF spectrum can be subtracted. The net XeF spectra measured at scattering angles of $\theta = 75°$ and 60° and for a coverage range of 0–0.22 monolayer (ML) F atom are shown in Fig. 1. The direct detection of the scattered XeF radical, before it undergoes a secondary, identity changing collision, is clear evidence for the abstraction mechanism.

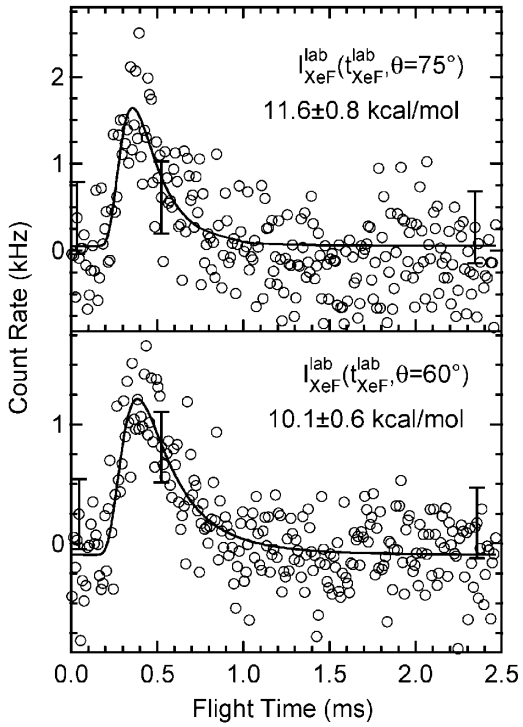

FIG. 1. Net XeF signal at $m/e = 148$ versus flight time measured at $\theta = 75°$ and 60°. Error bars represent the propagated statistical uncertainty. The solid line is a fit to a Maxwell-Boltzmann function [2] from which average energies shown ($\pm 2\sigma$) are obtained.

The intriguing observation is the detection of F atoms in the gas phase. Figure 2 shows the F atom TOF spectra at $m/e = 19$, I_F^{lab} (t_F^{lab}, $\chi_F = 75°$ and 60°) that have been corrected for the small contribution from dissociative ionization of the unreactively scattered XeF_2 to F^+. Unlike the XeF signal at $m/e = 148$, the F signal at $m/e = 19$ has a second contribution: the dissociative ionization of XeF to produce F^+. Unfortunately, the lack of a XeF radical beam precludes measurement of a cracking ratio that could then be used to subtract the contribution of XeF dissociative ionization to F^+. However, eight TOF spectra spanning a coverage range of 0 to 1.25 ML were measured at each of three scattering angles. With this amount of data, it is possible to increase the F^+/XeF^+ cracking ratio until a value is found that makes the F signal be zero at some flight time when the contribution from the dissociative ionization of XeF to F^+ is subtracted from one of the spectra such as shown in Fig. 2. This value is thus the maximum physically possible value for the cracking ratio. It is determined to be 0.4 and is limited by the $m/e = 19$ TOF spectrum measured at a scattering angle of $\chi_F = 75°$ and a coverage range of 0.88–1.25 ML F. The $m/e = 148$ TOF spectrum multiplied by this ratio has been subtracted from the raw $m/e = 19$ TOF spectrum to yield the net F atom spectra shown in Fig. 2. The observation of F atoms suggests that some XeF dissociates in the gas phase prior to reaching the detector. Given the weak XeF bond strength, 3 kcal/mol, relative to the 81 kcal/mol exothermicity of the abstraction reaction [11], a small fraction of the reaction exothermicity channeled into the XeF internal modes would readily lead to dissociation.

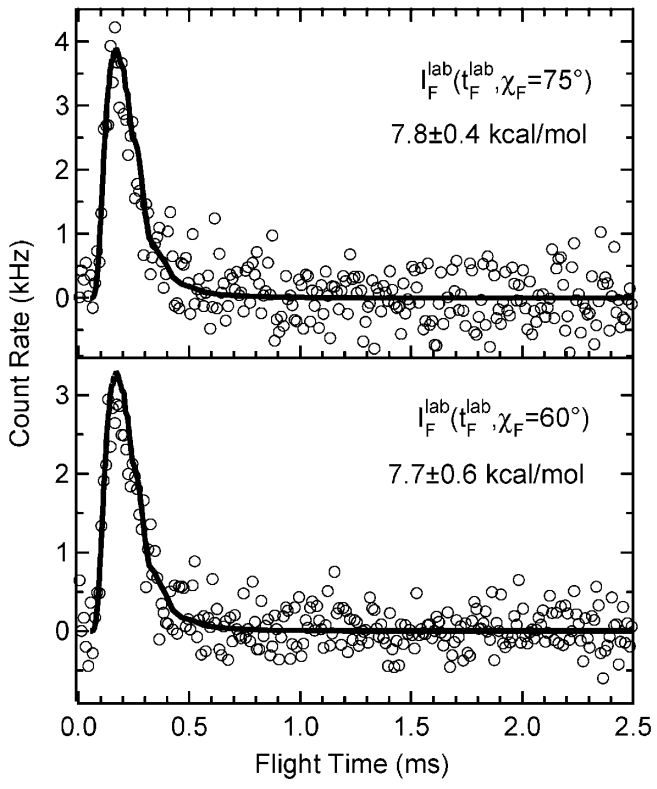

FIG. 2. Net F signal at $m/e = 19$ versus flight time measured at $\chi_F = 75°$ and 60°. Average energies with $\pm 2\sigma$ uncertainty are shown. The solid line is simulated result.

If the F atoms are the result of the dissociation of XeF in the gas phase, then there must be an equivalent number of Xe atoms whose TOF spectra are dictated by conservation of the XeF momentum and energy. That is, the momentum of the Xe atom resulting from XeF dissociation must be balanced by an equal and opposite momentum of the F atom, and its energy must be the difference between the energy of XeF above its dissociation limit and the translational energy of the F atom. In the center of mass coordinate system, the conservation equations are

$$m_{Xe}\vec{v}_{Xe}^{c.m.} = -m_F\vec{v}_F^{c.m.}, \tag{1}$$

$$\begin{aligned}\tfrac{1}{2}m_{Xe}|\vec{v}_{Xe}^{c.m.}|^2 + \tfrac{1}{2}m_F|\vec{v}_F^{c.m.}|^2 &= E_{int}(XeF) - E_{diss}(XeF)\\ &= E_{c.m.},\end{aligned} \tag{2}$$

where m is the mass and $\vec{v}_F^{c.m.}$ is the center of mass velocity of the designated species, E_{int} is the internal energy of XeF, and E_{diss} is the XeF bond dissociation energy. The center of mass energy, $E_{c.m.}$, is the XeF internal energy that is converted to the translational energy of the Xe and F atoms upon XeF dissociation. Solving for the center of mass velocities yields

$$|\vec{v}_F^{c.m.}| = \sqrt{\frac{2E_{c.m.}}{m_F(1+\frac{m_F}{m_{Xe}})}}, \qquad |\vec{v}_{Xe}^{c.m.}| = \sqrt{\frac{2E_{c.m.}}{m_{Xe}(1+\frac{m_{Xe}}{m_F})}}. \tag{3}$$

Since $\vec{v}_F^{c.m.}$ can be determined from the measured F atom TOF spectra, $E_{c.m.}$ can be determined from the first equality in Eq. (3). In turn, $E_{c.m.}$ is used to predict $\vec{v}_{Xe}^{c.m.}$, and those predictions are compared to the measured Xe atom TOF spectra. If dissociation of XeF is a gas phase process, then the predicted Xe spectra must agree well with those measured.

The procedure is as follows. The F atom center of mass velocity is related to its laboratory velocity, $\vec{v}_F^{lab}$, by the velocity of scattered XeF, $\vec{v}_{XeF}$, as shown in the Newton diagram in Fig. 3. The flux distribution of F atom laboratory velocities, $I_F^{lab}(v_F^{lab}, \chi_F)$, which are measured as number density TOF spectra at various laboratory scattering angles, χ_F, such as shown in Fig. 2, is related to the equivalent distribution [10] in the center of mass system, $I_F^{c.m.}(v_F^{c.m.}, \phi)$ by the Jacobian, $(v^{lab}/v^{c.m.})^2$:

$$\begin{aligned}I_F^{lab}(v_F^{lab}(v_{XeF}), \chi_F(\theta)) &= \left(\frac{v_F^{lab}}{v_F^{c.m.}}\right)^2 I_F^{c.m.}(v_F^{c.m.}(E_{c.m.}), \phi)\\ &= \frac{(v_F^{lab})^2}{v_F^{c.m.}} I(E_{c.m.})I(\phi),\end{aligned} \tag{4}$$

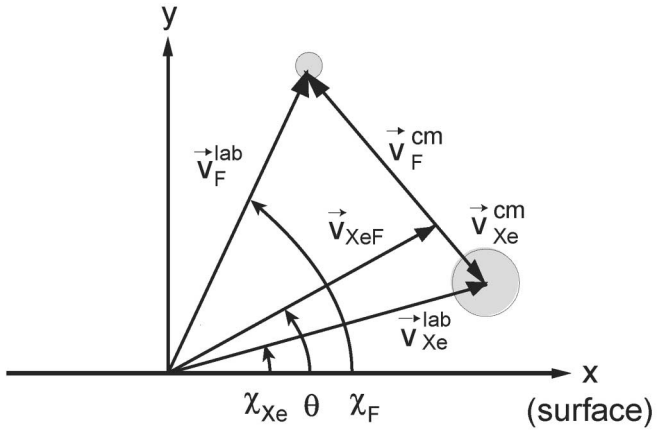

FIG. 3. Newton diagram relating center of mass and laboratory frame velocity vectors for gas phase dissociation of XeF.

where θ is the angle that XeF scatters from the surface, and ϕ is the angle of the XeF molecular axis with respect to $\vec{v}_{XeF}$. The second equality in Eq. (4) relates the center of mass velocity distribution to an energy distribution via the Jacobian $v^{c.m.}$ and shows the center of mass energy distribution, $I_F^{c.m.}(E_{c.m.}, \phi)$, approximated as the product of $I(\phi)$, the probability that XeF dissociates at axis orientation ϕ, and $I(E_{c.m.})$ [10].

The distributions $I(E_{c.m.})$ and $I(\phi)$ are determined by performing a forward convolution calculation using Eq. (4), the left hand equality of Eq. (3), and the Newton diagram, along with the measured velocity and angular distributions of XeF to predict $I_F^{lab}(v_F^{lab}, \chi_F)$, the laboratory velocity distribution of the F atom flux at some scattering angle. The velocity distribution in turn is transformed into a number density distribution in time that can be compared directly with the TOF spectrum. The functional forms of $I(E_{c.m.})$ and $I(\phi)$ or each of their single parameters are adjusted, and the forward convolution calculation is carried out iteratively until good agreement is attained. The optimal form of $I(E_{c.m.})$ is determined to be $I(E_{c.m.}) = (RT)^{-1} \exp(-E_{c.m.}/RT)$ where $T = 1970$ K. The optimal form of $I(\phi)$, the probability that XeF dissociates at a bond axis orientation ϕ, is determined to be one for XeF axes oriented within $\pm 120°$ from the normal with the F end pointing away from the surface and zero for other orientations. The predicted F atom TOF spectra, which are the result of 8×10^6 trajectories of $\{\phi, \theta, \vec{v}_{XeF}, E_{c.m.}\}$, are shown as solid lines in Fig. 2. The simulated spectrum at $\chi_F = 75°$ is normalized at one point (the maximum intensity) of the spectrum measured at 75°. This same normalization factor is used to obtain the intensities of the simulated spectra at 60° and 30°. The agreement between the simulated and measured spectra is excellent at all angles.

The same distributions, $I(E_{c.m.})$ and $I(\phi)$, are used in the forward convolution calculation of Eq. (4), along with the right hand equality of Eq. (3), the Newton diagram, and the measured velocity and angular distributions of XeF to predict the distribution of laboratory velocities of the Xe atoms, $I_{Xe}^{lab}(v_{Xe}^{lab}, \chi_{Xe})$. The predicted distributions are transformed into number density distributions in time and are shown as thick solid lines in Fig. 4. Because one Xe atom is produced for every F atom, the intensity of the simulated spectra is normalized so that the flux of Xe atoms integrated over all scattering angles is equal to the angle integrated flux of F atoms. The difference in the ionization probabilities and transmission functions of Xe and F in the detector are taken into account. As can be seen, the simulation predicts Xe atoms to be produced at flight times where Xe atoms are observed. It identifies the Xe feature at the shortest flight times as arising from the dissociation of XeF in the gas phase. In addition, the simulation, on the basis of conservation of mass, predicts the Xe atom intensity accurately.

However, not only does the dissociation of XeF contribute to the Xe spectrum, but two atom adsorption also contributes. That is, the complementary XeF radical may

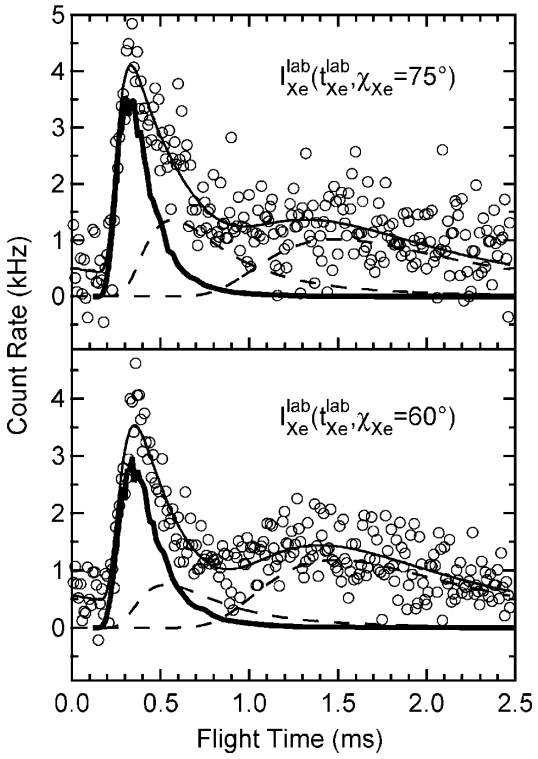

FIG. 4. Net Xe signal at $m/e = 167$ versus flight time at $\chi_F = 75°$ and 60°. Maximum value, as described for F^+, used for XeF dissociative ionization to Xe^+. Thick solid line is the simulated result. Uncertainty in the ordinate of the simulated result is ±22%, due primarily to the 20% uncertainty in the F atom ionization cross section. Dotted lines are Maxwell-Boltzmann fits (average energies are 4.2 and 0.7 at $\chi_F = 75°$ and 4.8 and 0.7 kcal/mol at $\chi_F = 60°$) to Xe resulting from two atom adsorption. Thin solid line is the sum of the three components.

interact a second time with the surface, as opposed to being scattered from the surface, allowing the F atom on XeF to be abstracted by the Si. The consequence is the liberation of a Xe atom in the gas phase. The Xe may be scattered into the gas phase immediately or it may subsequently equilibrate thermally with the crystal and eventually desorb. Indeed, the longest time feature is well fit by a Maxwell-Boltzmann distribution at the surface temperature, 150 K. In either case, the Xe atom produced as a result of two atom adsorption does not scatter into the gas phase with the same energy and dynamics as a Xe atom produced by gas phase dissociation of XeF. The TOF spectra in Fig. 4 clearly exhibit three features, indicative of multiple routes for Xe production.

Physically, $I(E_{\mathrm{c.m.}})$ is the internal energy of XeF above its dissociation limit. It has an average value of 3.9 ± 0.7 kcal/mol. The uncertainty is obtained by varying the average $E_{\mathrm{c.m.}}$ until it produces a noticeably poorer fit to the F atom TOF spectra. Because $I(E_{\mathrm{c.m.}})$ peaks near zero energy, the internal excitation is attributed to rovibrational excitation of the ground electronic state of XeF [12]. Excitation into the vibrational continuum necessitates dissociation within a vibrational period. This knowledge, coupled with the known XeF velocity, implies that XeF dissociates within 2 Å from the abstraction site. Simulations carried out for XeF dissociation when the bond axis is oriented with the F end pointing towards the surface ($\pm$ 120°–180° between the XeF bond and the surface normal) do not reproduce the F atom TOF spectra as well. The limitation on the XeF bond orientation is physically reasonable given the linear geometry of XeF_2 as it approaches the transition state and the inability of XeF to rotate in the short time between abstraction and dissociation. For the data shown here, an average of 11 and 7 kcal/mol of the 81 kcal/mol abstraction reaction exothermicity are partitioned to translational and rovibrational energy, respectively.

In summary, conservation of energy, momentum, and mass accurately predict the angle-resolved Xe atom TOF spectra based on knowledge of the angle-resolved TOF spectra of the scattered F atom and the XeF fragment. This excellent agreement resulting from a two body treatment of this system implies dissociation of XeF in the gas phase, unperturbed by the presence of a third body, the nearby surface. Knowledge and inclusion of atom abstraction and gas phase dissociation of a surface reaction product are critical to the development of accurate kinetic models for semiconductor etching, heterogeneous catalysis, and chemical vapor deposition.

This work is supported by NSF CHE-0091810.

[1] Y. L. Li, D. P. Pullman, J. J. Yang, A. A. Tsekouras, D. B. Gosalvez, K. B. Laughlin, Z. Zhang, M. T. Schulberg, D. J. Gladstone, M. McGonigal, and S. T. Ceyer, Phys. Rev. Lett. **74**, 2603 (1995).

[2] M. R. Tate, D. B. Gosalvez, D. P. Pullman, A. A. Tsekouras, Y. L. Li, J. J. Yang, K. B. Laughlin, S. C. Eckman, M. F. Bertino, and S. T. Ceyer, J. Chem. Phys. **111**, 3679 (1999).

[3] M. R. Tate, D. P. Pullman, Y. L. Li, D. Gosalvez-Blanco, A. A. Tsekouras, and S. T. Ceyer, J. Chem. Phys. **112**, 5190 (2000).

[4] A. Mödl, H. Robota, J. Segner, W. Vielhaber, M. C. Lin, and G. Ertl, Surf. Sci. **169**, L341 (1986).

[5] D. J. Driscoll, W. Martir, J.-X. Wang, and J. H. Lunsford, J. Am. Chem. Soc. **107**, 58 (1985).

[6] E. R. Behringer, H. C. Flamm, D. J. Sullivan, D. P. Masson, E. J. Lanzendorf, and A. C. Kummel, J. Phys. Chem. **99**, 12 863 (1995).

[7] S. T. Ceyer, D. J. Gladstone, M. McGonigal, and M. T. Schulberg, *Physical Methods of Chemistry*, edited by B. W. Rossiter and R. C. Baetzold (Wiley, New York, 1993), 2nd ed., Vol. IXA, p. 383.

[8] D. P. Pullman, A. A. Tsekouras, Y. L. Li, J. J. Yang, M. R. Tate, D. B. Gosalvez, K. B. Laughlin, M. T. Schulberg, and S. T. Ceyer, J. Phys. Chem. B **105**, 486 (2001).

[9] J. R. Holt, R. C. Hefty, M. R. Tate, S. C. Eckman, M. F. Bertino, and S. T. Ceyer, J. Phys. Chem. B **106**, 8399 (2002).

[10] Y. T. Lee, *Atomic and Molecular-Beam Methods*, edited by G. Scoles (Oxford University Press, Oxford, 1988), Vol. I, p. 553.

[11] The exothermicity of the F atom abstraction reaction of XeF_2 with a Si dangling bond is calculated as 81 kcal/mol using bond enthalpies of 60 kcal/mol for the first F-XeF bond [P. C. Tellinghuisen *et al.*, J. Chem. Phys. **68**, 5187 (1978)], 7 kcal/mol for π bond energy of Si dimers [M. P. D'Evelyn *et al.*, J. Chem. Phys. **96**, 852 (1992); U. Hofer *et al.*, Phys. Rev. B **45**, 9485 (1992)], and 148 kcal/mol for the F-Si bond [C. J. Wu *et al.*, Phys. Rev. B **45**, 9065 (1992)].

[12] R. D. Levine and R. B. Bernstein, *Molecular Reaction Dynamics and Chemical Reactivity* (Oxford University Press, New York, 1987).